TRYPTOPHAN METABOLITES ARE ASSOCIATED WITH GUT-BRAIN ALTERATIONS IN FUNCTIONAL DYSPEPSIA

Authors

Matthias Ceulemans[1,2], Lucas Wauters[1,3], Nathalie Weltens[1,4,5], Greet Vandermeulen[1], Henriette de Loor[6], Pieter Evenepoel[6,7], Raul Y. Tito[8,9], Arnau Vich Vila[8,9], Muriel Derrien[8,9], Boushra Dalile[10], Jan Tack[1,3], Kristin Verbeke[1], Jeroen Raes[8,9,#], Lukas Van Oudenhove[1,4,5,#], Tim Vanuytsel[1,3,#,*]

Affiliations

1) Translational Research Center for Gastrointestinal Disorders (TARGID), Department of Chronic Diseases and Metabolism (ChroMeta), KU Leuven, Leuven, Belgium

2) Precision Immunology Institute, Icahn School of Medicine at Mount Sinai, New York, NY

3) Gastroenterology and Hepatology, University Hospitals Leuven, Leuven, Belgium

4) Laboratory for Brain-Gut-Axis Studies (LaBGAS), KU Leuven, Leuven, Belgium

5) Leuven Brain Institute, KU Leuven, Leuven, Belgium.

6) Nephrology and Renal Transplantation Research Group, Department of Microbiology, Immunology and Transplantation, KU Leuven, Leuven, Belgium

7) Nephrology and Renal Transplantation, University Hospitals Leuven, Leuven, Belgium

8) Laboratory of Molecular Bacteriology, Department of Microbiology, Immunology and Transplantation, Rega Institute, KU Leuven, Leuven, Belgium.

9) Center for Microbiology, Vlaams Instituut voor Biotechnologie (VIB), Leuven, Belgium.

10) Laboratory of Biological Psychology, KU Leuven, Belgium

# Senior authors contributed equally

* Correspondence to: Tim Vanuytsel, MD, PhD, University Hospitals Leuven, Herestraat 49, 3000 Leuven, Belgium. e-mail: tim.vanuytsel@uzleuven.be

Uploaded as a preprint on MedRxiv: https://doi.org/10.1101/2025.11.23.25340799

Short title: Altered metabolites and gut-brain axis in FD

Conflict of interest statement: The authors disclose no conflicts.

Data availability statement: The raw data generated and analyzed during the current study are available from the corresponding author upon reasonable request.

Abstract

Background and aims Disturbances in the microbiota-gut-brain axis are thought to contribute to the pathophysiology of disorders of gut-brain interaction, including functional dyspepsia (FD), although comprehensive human data remain scarce. We aimed to study the relationships among microbiota-produced metabolites including tryptophan metabolites and short-chain fatty acids (SCFA), and functional brain connectivity in FD, in relation to symptomatology.

Methods In 46 patients with Rome IV-diagnosed FD and 30 healthy controls (HC), targeted metabolomics using chromatography and mass spectrometry was conducted to quantify metabolites in blood, urine, and stool. Associations with gut microbiota and symptomatology were tested using fecal quantitative microbiota profiling and validated symptom questionnaires. Resting-state functional magnetic resonance imaging in 27 patients and 36 HC enabled analysis of functional connectivity in selected brain networks.

Results Patients with FD exhibited distinct profiles of tryptophan metabolites and SCFA with higher urinary indole-3-acetate (IAA, P=0.018), lower serum kynurenine (P=0.030) and lower plasma propionate (P=0.0055) concentrations. FD-specific metabolite alterations were associated with more severe GI and psychological symptoms. The fecal microbiota profile was similar between FD and HC. Complementary analyses demonstrated significant alterations in resting-state brain connectivity of 44 predefined regions between FD and HC, while a connectivity-based classifier discriminated FD from HC (82.3% sensitivity, 66.7% specificity, P<0.0001). Differences in connectivity measures mediated the higher urinary IAA levels in FD.

Conclusion Dysregulated functional brain connectivity supports an objective pathophysiology in FD. Alterations in specific tryptophan metabolite and SCFA levels were linked to symptomatology, highlighting their potential as biomarkers, and warranting further investigation on microbiota modulating therapies for FD.

ClinicalTrials.gov (www.clinicaltrials.gov): NCT03545243

Keywords: Functional dyspepsia; microbiota-gut-brain axis; indole-3-acetate; short-chain fatty acids; gastrointestinal microbiome

Introduction

Functional dyspepsia (FD) is a chronic condition characterized by specific meal-related and painful symptoms perceived in the gastroduodenal region. Diagnosed by the Rome IV criteria in the absence of any organic or structural disease, hallmark FD symptoms include postprandial fulness, early satiation, epigastric pain and burning[1]. With an estimated worldwide prevalence of over 7%, FD affects considerably more individuals than irritable bowel syndrome (IBS)[2], despite more limited public awareness in comparison. Both functional gastrointestinal (GI) disorders were recently relabeled as disorders of gut-brain interaction (DGBI)[3], to better reflect their pathophysiology, presumed to involve dysfunction of intricate gut-brain interplay. Besides an impaired quality of life[4] and common overlap with psychological distress[5], FD imposes a substantial socio-economic burden due to repeated healthcare visits and a lack of cost-effective treatment options[6], highlighting the pressing need for increased insight in its pathophysiology to support clinical diagnosis and guide therapy selection.

Research on pathophysiological mechanisms underlying FD symptoms has primarily focused on mucosal immune activation[7], epithelial barrier defects[8] and gut microbial alterations[9]. Specific microbial shifts were found in the proximal GI tract[10], with most evidence for duodenal microbial changes, including increased abundance of *Streptococcus*[10] and reduced *Firmicutes*[11], *Neisseria*[12] and *Porphyromonas*[12] abundance in FD compared to controls. An independent association between the onset of FD and psychological disorders such as anxiety and mood disorders suggests an important role of gut-brain communication[13]. This gut-brain crosstalk can potentially be influenced by the gut microbiota. Important metabolites produced by gut microbes, most notably short-chain fatty acids (SCFA) and aromatic amino acid (AAA; tryptophan, phenylalanine and tyrosine) metabolites, are thought to directly or indirectly play a role in various homeostatic processes including microbiota-gut-brain communication[14, 15]. Indole-3-acetate (IAA), a gut microbiota-derived tryptophan metabolite, has been shown to relay psychological stress to the gut in mice[16], offering an attractive hypothesis for the high psychological symptom burden in FD and related DGBI. However, comprehensive data on the role of microbial metabolites in altered microbiota-gut-brain crosstalk in FD are currently lacking.

To address this knowledge gap, we performed targeted metabolomic and fecal microbiota profiling in a prospectively recruited cohort of patients with FD and matched healthy controls (HC). We combined extensive symptom profiling and functional magnetic resonance imaging (fMRI) of the brain to evaluate central alterations related to FD pathophysiology. Lastly, using

regression, classification and mediation models, we identified a link between urinary IAA, GI and psychological symptom profiles, and functional brain alterations in FD.

Methods

Study design and participants

Patients with Rome IV-defined FD (n=46) and matched healthy controls (HC) (n=30) were prospectively recruited in a single center to undergo sampling of blood, urine and feces for extensive metabolite and microbiota profiling. In- and exclusion criteria are listed in the **Supplementary Methods**. During the study visit, participants completed validated questionnaires assessing GI and extraintestinal symptoms (**Supplementary Methods**). The study was approved by the University Hospitals / KU Leuven Ethics Committee for Research (S60953, S60984) and registered at ClinicalTrials.gov (NCT03545243). All participants provided written informed consent before the start of the study. The study was conducted in accordance with the Declaration of Helsinki and the Guidelines for Good Clinical Practice. All co-authors had access to the study data and have reviewed and approved the final manuscript.

Sample collection

During study visits, qualified staff collected blood samples in fasted state (≥ 6h) in EDTA and SST tubes (both BD Vacutainer) for plasma and serum collection, respectively. Blood samples were centrifuged, aliquoted, and serum (amino acid metabolite analyses) and plasma (short-chain fatty acids (SCFA) analyses) were stored at -80°C until further processing. Participants provided a fasted spot urine sample, which was stored at -80°C until analysis. Within two days of the study visit, participants collected a stool sample at home in a container provided for this purpose, which was immediately frozen (-18°C) at participants' own freezer and transported to the lab with ice packs, where samples were stored at -80°C until analysis. Participants scored the consistency of their stool sample using the Bristol Stool Scale (BSS) as a proxy for intestinal transit time[17]. A subset of participants underwent resting state functional magnetic resonance imaging (rs-fMRI) as part of the study.

Targeted metabolite analyses

A validated panel of aromatic amino acids (AAA), host and microbial AAA metabolites, and uremic toxins (**Figure 2A**) was quantified via ultra-performance liquid chromatography-tandem mass spectrometry as previously published[18] on spot urine samples and fasted serum samples. Creatinine was measured in urine samples via routine enzymatic assay, and urinary metabolite concentrations were normalized to creatinine levels to mitigate dilution effects. Measurement of SCFA was performed as previously described following optimized

gas chromatography-mass spectrometry protocols for frozen fecal[19] and fasted plasma samples[20].

Functional magnetic resonance imaging

Optional rs-fMRI and T1 structural MRI measurements were performed in consenting individuals (27 patients with FD and 20 HC) at the University Hospitals Leuven Radiology Department using a 3T Philips Achieva DStream MRI scanner (32-channer head coil). The dataset was complemented with rs-fMRI measurements of a previously recruited cohort of 16 additional HC who underwent identical fMRI procedures (same scanner, same head coil, identical acquisition parameters). Processing and analysis of fMRI data was performed in batch and described in the **Supplementary Methods**.

Statistical analyses

Statistical analyses were performed in R (v4.5.1) and described in detail in the **Supplementary Methods**.

Results

High psychological symptom burden in FD

To investigate the contribution of gut microbial metabolites to the pathophysiology of FD, we studied a well-characterized cohort of 46 patients with Rome IV-diagnosed FD and 30 HC. The absence of endoscopic alterations was confirmed during esophagogastroduodenoscopy in all participants. The characteristics of this cohort have been described before[21] (**Supplementary Table 1**). Briefly, patients and controls were matched for age, sex, body mass index (BMI), and geographic origin (all $P > 0.1$). Thirty nine percent of patients with FD (n = 18/46) were taking PPI at the time of sampling, while none of the HC were taking PPI. As reported before[12], food frequency questionnaires revealed differences in dietary patterns between study groups, with lower estimated intake of fiber ($\eta_p^2 = 0.12$, $P = 0.015$, $q_{FDR} = 0.045$) and protein ($\eta_p^2 = 0.21$, $P = 0.0012$, $q_{FDR} = 0.0071$) in FD compared to HC. Intake of other macronutrients and total energy intake was similar in FD (all $P > 0.1$) (**Supplementary Table 2**). Besides more severe GI-specific symptoms (LPDS and PAGI-SYM; both $q_{FDR} < 0.0001$), patients with FD presented with significantly higher symptom scores for anxiety (GAD7), perceived stress (PSS), depression (PHQ9), extraintestinal symptoms (PHQ12), GI-specific anxiety (VSI) and posttraumatic stress (PTSD) (all $q_{FDR} < 0.0005$) (**Figure 1**, **Supplementary Table 3**, **Supplementary Results**) as described before[5].

Patients with FD exhibit a distinct metabolite profile

We measured the concentrations of a relevant selection of host and microbiota-derived aromatic amino acids (AAA) and key AAA metabolites (**Figure 2A**) using targeted ultra-performance liquid chromatography-tandem mass spectrometry. First, we looked at the overall serum metabolite composition. Principal component analysis (PCA) and permutational analysis of variance (PERMANOVA) revealed a significantly distinct serum-derived metabolic signature between FD and HC ($R^2 = 0.031$, $P_{PERMANOVA} = 0.012$) (**Figure 2B**). When only including microbial AAA metabolites, the serum metabolite signature was again different between FD and HC ($R^2 = 0.033$, $P_{PERMANOVA} = 0.030$) (**Supplementary Figure 1A**). The urinary AAA metabolite profile was not different between both groups ($R^2 = 0.024$, $P_{PERMANOVA} = 0.11$) (**Supplementary Figure 1B**). However, similarly to the serum results, the profile of microbial AAA metabolites in urine differed significantly between FD and HC ($R^2 = 0.037$, $P_{PERMANOVA} = 0.040$) (**Figure 2C**).

Next, the concentrations of analyzed molecules were standardized and aggregated by their origin, i.e. AAA, host-derived AAA metabolites and microbial AAA metabolites (**Figure 2A**), to assess differences in metabolites based on their origin. To mitigate the potential confounding effects of dietary or PPI intake, all models were adjusted for protein intake and PPI use.

Serum (η_p^2 = 0.10, P = 0.027) but not urinary host AAA metabolites (η_p^2 = 0.00004, P = 0.97) were lower in FD (**Figure 2D-E**). In line with PCA results presented before, urinary microbial AAA metabolite levels (η_p^2 = 0.11, P = 0.033) were higher in FD (**Figure 2E**). After multiple testing correction the differences in metabolite groups (serum host-derived AAA metabolites: q_{FDR} = 0.081, urinary microbial AAA metabolites: q_{FDR} = 0.098) remained trends. Interestingly, protein intake was associated with serum microbial AAA metabolite levels (η_p^2 = 0.12, P = 0.017) but not with urinary levels, nor with host AAA metabolite levels in serum or urine. Systemic and urinary AAA levels were similar between groups (all P > 0.1) (**Figure 2D-E**). On the individual metabolite level, serum host-derived AAA metabolite alterations were driven by lower serum kynurenine (Kyn) (η_p^2 = 0.10, P = 0.030, q_{FDR} = 0.060), while urinary phenylacetylglutamine (PAGln) (η_p^2 = 0.12, P = 0.030, q_{FDR} = 0.080) and indole-3-acetate (IAA) (η_p^2 = 0.14, P = 0.018, q_{FDR} = 0.080) were among elevated urinary microbial AAA metabolites in FD (**Figure 2F**). Higher serum phenylalanine (η_p^2 = 0.09, P = 0.038, q_{FDR} = 0.11) and PAGln (η_p^2 = 0.09, P = 0.043, q_{FDR} = 0.34) levels if FD did not persist after multiple testing correction (**Figure 2F**).

SCFA are key metabolites produced by the gut microbiota from carbohydrate fermentation. Fecal and plasma main SCFA (acetate, butyrate, propionate) were analyzed using gas chromatography-mass spectrometry. Concentrations of all measured individual and total SCFA in both feces and plasma were on average lower in FD compared to HC (**Figure 3A-B**). Lower systemic levels of propionate (η_p^2 = 0.16, P = 0.0055, q_{FDR} = 0.011) and total SCFA (η_p^2 = 0.17, P = 0.0044, q_{FDR} = 0.011) reached statistical significance, independent of PPI and fiber intake, the major substrate for SCFA production (**Figure 3B**).

IAA, Kyn and propionate are associated with gastrointestinal and comorbid psychological symptoms in FD

Gut microbiota-derived IAA was recently shown to relay psychological stress to the gut in mice, while increased IAA levels in patients with major depressive disorder demonstrated its relevance in a human context[16]. Therefore, we subsequently interrogated whether the distinct metabolic profile in patients with FD, including increased urinary IAA levels, was associated with the characteristic symptom profile in FD.

To explore the clinical relevance of altered metabolites, we performed correlation analyses between symptom outcomes and all measured metabolites in this cohort. Consistently, urinary IAA, plasma propionate and serum Kyn were among the metabolites most strongly associated with symptomatology (**Figure 4A**, **Supplementary Table 4**). To confirm these exploratory correlations, we constructed linear regression models to assess associations between IAA, propionate and Kyn, with participants' GI and comorbid psychological

symptoms. Urinary IAA was associated with general anxiety, depression, extraintestinal and GI-specific (LPDS) symptoms in a univariable model (**Figure 4B**, **Supplementary Table 5**), confirming the previously suggested link between IAA and psychological distress[16]. Plasma propionate levels were significantly and inversely associated with symptom levels except for perceived stress (**Figure 4C**, **Supplementary Table 5**). Similarly, serum Kyn, a tryptophan metabolite of non-microbial origin, was inversely associated with symptoms except for GI-specific anxiety (**Figure 4D**, **Supplementary Table 5**). Medium to large effect sizes of these metabolite-symptom associations persisted when controlling for dietary protein (IAA, Kyn) or fiber (propionate) and PPI intake (**Supplementary Table 6**), suggesting independent associations.

Of note, urinary IAA, plasma propionate and serum Kyn were only minimally correlated with each other, suggesting their associations with symptoms might be independent (**Figure 4E**). To assess the individual contribution of each metabolite of interest on the different symptom variables, we used multiple linear regression analysis with correction for fiber and protein intake. While urinary IAA was strongly associated with depression, extraintestinal and general GI symptoms, the association between plasma propionate with upper-GI symptoms, general and GI-specific anxiety, and both positive and negative affect had the highest effect sizes. In contrast, serum Kyn only contributed minimally to each of the metabolite-symptom associations (**Figure 4F**, **Supplementary Table 7**).

To investigate whether the shifts in specific metabolites were linked to alterations in the gut microbiota, we performed quantitative microbiota profiling (QMP) on fecal samples, combining 16S rRNA gene sequencing with flow cytometric quantification of microbial cell counts[22]. Despite similar stool consistency and microbial density, diversity or composition between FD and HC (**Figure 5A-E**, **Supplementary Results**), the quantitative abundance of select taxa (decreased *Odoribacter*, *Turicibacter* and unclassified *Clostridia*; increased *Flavonifractor*; all q_{FDR} = 0.075) tended to differ in patients with FD (**Figure 5D**, **Supplementary Results**). These changes were independent of PPI intake and intestinal transit time, although transit time was linked to a higher number of differentially abundant fecal genera compared to FD diagnosis or PPI intake variables (**Figure 5D**). In addition, the fecal genera associated with metabolic changes and psychological symptom profiles clustered separately, suggesting the absence of a shared microbial signature underlying these alterations in FD (**Supplementary Figure 3**, **Supplementary Results**).

Resting-state functional connectivity in salience, emotional-arousal, and central autonomic brain networks is altered in FD and classifies FD and HC with reasonable accuracy

Gut microbiota metabolites have been proposed as key contributors to microbiota-gut-brain interplay, which is thought to be a major driver underlying disorders of gut-brain interactions such as FD. However, studies that comprehensively consider these metabolite and brain components are scarce. Therefore, participants in this study underwent optional resting-state functional magnetic resonance imaging (rs-fMRI) of the brain, completed by 27 patients with FD and 20 HC, supplemented with data from 16 additional HC who underwent identical rs-fMRI procedures. This cohort of 36 HC had a similar sex distribution compared to the 27 FD patients (25 females (69%) vs 22 females (81%), P = 0.38) but was younger on average (mean age (years) ± standard deviation age: 28 ± 9 years vs 34 ± 12, P = 0.015).

Multivariate general linear model (GLM) analyses of a region-of-interest (ROI)-to-ROI connectivity matrix incorporating 44 a priori selected ROIs involved in salience, emotional-arousal and central autonomic networks[23] (**Supplementary Table 8**), demonstrated a significant difference in connectivity between FD and HC for the right inferior frontal gyrus - pars triangularis (ventrolateral prefrontal cortex, vlPFC) (ROI mass = 61.27, P = 0.0013, P_{FWE} = 0.046). This was driven by significantly stronger connectivity between this region with the bilateral rostral anterior cingulate cortex and gyrus rectus, as well as with left medial fronto-orbital gyrus and superior frontal gyrus in FD versus HC (**Figure 6A**, **Supplementary Table 9**).

Next, we applied functional connectivity multivariate pattern analysis (fc-MVPA) as a whole-brain data-driven approach to identify regions in which connectivity with the rest of the brain differs between FD and HC. A significant between-group difference in whole-brain voxel-based connectivity was found for a cluster in the left vlPFC including frontal orbital cortex and inferior frontal gyrus - pars triangularis (peak MNI coordinates [x, y, z] = [-41, 33, -7]; k = 61 voxels; TFCE = 431.76; P = 0.001; P_{FWE} = 0.048) (**Figure 6B**). This difference was driven by stronger connectivity between this cluster and other (pre)frontal, inferior temporal, and cerebellar areas in FD patients (red), and stronger connectivity between this cluster and insular and parietal regions in HC (blue) (**Figure 6C**).

In addition to the differential pairwise connectivity relationships between groups, we applied graph theoretical analysis as a network-based approach and compared graph measures between FD and HC (FDR-corrected for 180 tests). Three out of the four global graph measures were significantly different between FD patients and HC ((M)ANOVA), with higher characteristic path length in HC, and higher efficiency and clustering coefficient in FD (**Supplementary Table 10**). For between-group analysis in nodal graph measures using (M)ANOVA, significant differences were found for characteristic path length in 30/44 ROIs,

for betweenness centrality in 3/44 ROIs, for clustering coefficient in 20/44 ROIs, and for efficiency in 27/44 ROIs (**Supplementary Table 10**).

To test the collective ability of the calculated graph measures to discriminate between patients with FD and controls, they were entered as independent variables in partial least squares discriminant analysis (PLS-DA). PLS-DA with all 540 graph measures as X variables and group (FD versus HC) as Y variable was performed and 5-fold cross-validation suggested a 1-factor solution with 55% of X variables (296/540) exceeding the variable importance plot (VIP) threshold of 0.8 (van der Voet $T^2 = 0$, $Q^2 = 0.18$) (**Supplementary Figure 4A**). The model cumulatively explained 25.3% and 33.3 % of the variance for the X variables and the Y variable, respectively (**Supplementary Table 11**). Classification performance was adequate and significantly different from chance (75.5% accuracy, 82.3% sensitivity, 66.7% specificity, area under the curve = 0.745, $P < 0.0001$) (**Figure 6D**).

Altered resting-state functional brain connectivity mediates elevated urinary IAA levels in FD

Partial least squares (PLS) regression with all 540 graph measures as X variables and urinary IAA as Y variable was performed and leave-one-out cross-validation suggested a 2-factor solution with 59% of X variables (320/540) exceeding the VIP threshold of 0.8 (van der Voet $T^2 = 0$, $Q^2 = 0.04$) (**Supplementary Figure 4B**). The model cumulatively explained 26.8% and 81.5% of the variance for the X variables and the Y variable, respectively (**Supplementary Table 12**). Moreover, the PLS regression model significantly predicted urinary IAA levels, explaining 81.1% of the variance (Pearson r = 0.90, $P < 0.0001$) (**Supplementary Figure 4C**). In similar models with plasma propionate or serum Kyn as the Y-variable, the cross-validation procedure did not suggest any factors to retain (based on a minimum value for the root mean PRESS statistic for the null model), indicating that the X-variables (i.e. graph measures) did not explain any variance in the Y-variables (**Supplementary Figure 4D**).

Of note, one-way ANOVA revealed that the standardized first factor of the PLS regression model – explaining 14.9% of the variance in the graph measures – was significantly higher in FD (Cohen's d = 1.13, $P = 0.0008$), while the second factor explaining 11.9% of the variance was not different between groups (d = 0.29, $P = 0.42$) (**Supplementary Figure 4E**). This prompted us to test whether the group difference in urinary IAA levels was mediated by differences in graph measures. For this purpose, we fitted a mediation model with group as the independent (X) variable, the standardized first graph measures factor of the PLS regression model predicting urinary IAA as the mediator (M) variable, and the standardized urinary IAA levels as the dependent (Y) variable. The indirect effect of group on IAA through

the graph measures factor (path A*B) was significant (β ± SE = -0.29 ± 0.10; 95% bootstrapped CI = [-0.52, -0.11], *P* = 0.0045) while the direct effect of group on IAA (path C) was non-significant (-0.24 ± 0.13, [-0.55, 0.034], *P* = 0.071) (**Figure 6E**). The total effect of group on IAA was significant (-0.53 ± 0.14, [-0.82, -0.26], *P* = 0.0001), confirming that differences in brain-connectivity measures mediated the higher urinary IAA levels in FD.

Discussion

The bidirectional interplay between the gut microbiota and the central nervous system, known as the microbiota-gut-brain axis, is well established through preclinical and clinical studies[24-26]. Nevertheless, its role in DGBI including FD remains incompletely understood. Here, we provide novel evidence for dysregulated SCFA and tryptophan metabolism in FD in the absence of major microbial alterations, which was linked to a worsened GI and psychological symptom profile. Rs-fMRI-based analysis of functional connectivity between relevant brain regions involved in salience, emotional-arousal and central autonomic networks demonstrated significant differences between FD and HC. Moreover, the increase in urinary IAA, a microbial tryptophan metabolite, in patients with FD was statistically mediated by differential brain connectivity between FD and HC, pointing toward a brain-to-gut signaling pathway previously identified in rodents.

We identified a dysregulated metabolite signature in FD compared to HC, with a marked reduction in circulating kynurenine but increased urinary IAA levels. This suggests a shift in tryptophan metabolism from the host kynurenine pathway toward microbial indole production. Interestingly, *Lactobacillus murinus*-produced IAA has recently been demonstrated to relay psychological stress to the gut in mice, where it caused impaired stem cell differentiation. In patients with major depressive disorder (MDD), *Lactobacillus* abundance and fecal IAA levels were higher compared to controls[16]. In contrast, supplementation of IAA partially alleviated colitis in mice by restoring intestinal barrier function[27], suggesting differential effects of IAA depending on the inflammatory and genetic context or mouse model.

All major SCFA concentrations (acetate, butyrate and propionate) measured in the circulation and feces were numerically lower in FD compared to controls, with the reduction in systemic propionate levels being most pronounced and statistically significant. This finding is especially interesting given that SCFA – important products of microbial carbohydrate degradation – can influence central processes when reaching the systemic circulation[14]. Lower systemic SCFA levels are in line with recent findings of decreased circulating butyrate and propionate levels in patients with MDD[28], suggesting that limited SCFA availability is particularly linked with the central and psychological aspects of FD. In addition, higher plasma butyrate but not propionate levels at baseline could predict remission of MDD at follow-up, making SCFA attractive candidates to be evaluated as prognostic, predictive, and/or therapeutic biomarkers in psychiatric disorders, and potentially DGBI including FD.

Importantly, altered metabolite levels in FD correlated with patient-reported outcomes, including two different measures of GI symptoms and various psychological outcomes such as anxiety, depression and extraintestinal symptom burden. This underscores the relevance

of metabolite dysregulation in FD, although cause and consequence cannot be untangled from our cross-sectional analysis.

Despite significant shifts in metabolite profiles, we found no major perturbations in the density, diversity and composition of the fecal microbiota in FD. Previous studies on microbial alterations in FD focused on the gastroduodenal environment, consistently demonstrating increased abundance of typical upper-GI bacteria such as *Streptococcus*[9, 10]. However, as microbial density and, consequently, the production of microbial metabolites progressively increase more distal to the duodenum, alterations in the composition of the lower GI microbiota might still be indirectly involved in gastroduodenal and psychological symptom generation. A recent case-control study from South-Korea in 12 patients with FD found an overall similar fecal microbiota composition compared to 16 controls as assessed by alpha and beta diversity[29], which we corroborated in a larger cohort with a different geographical origin. Relative abundances of *Butyricicoccus* and *Faecalibacterium* – known butyrate producers – were reduced in FD, which is in line with our findings of lower SCFA concentrations in general, and a decreased abundance of the SCFA-producing genus *Odoribacter*. Of note, inverse associations between fecal *Fusicatenibacter* abundance and various psychological symptoms including PTSD are consistent with a reduction in *Fusicatenibacter saccharivorans* in Spanish individuals with comorbid depression, anxiety and PTSD symptoms in the post-COVID-19 pandemic setting[30].

To the best of our knowledge, this is the first study to demonstrate a reduction in SCFA levels in FD compared to HC. Nevertheless, we and others reported on the beneficial effects of probiotics for FD in randomized placebo-controlled trials, associated with proliferation of SCFA-producing microbes. A combination of two spore-forming *Bacillus* strains (*B. coagulans* MY01 and *B. subtilis MY02*) effectively reduced FD symptoms and increased the fecal abundance of butyrate-producing genera *Faecalibacterium* and *Roseburia* after 8 and 16 weeks of probiotic intervention[31]. More recently, a Chinese study in 200 patients with FD demonstrated superior symptom relief of a high-dose probiotic consisting of *Bifidobacterium animalis* subsp. *lactis* BL-99 compared to various control groups (placebo, low-dose probiotic, PPI treatment)[32]. Similarly, BL-99 probiotic intervention increased the abundance of multiple SCFA-producing microbes in stool, resulting in elevated fecal and systemic SCFA levels. This warrants further investigation on the anticipated beneficial effects of intervention with probiotics, as well as prebiotics, aimed at restoring circulating SCFA levels in randomized controlled trials.

One of the most intriguing findings of our study is the significantly altered brain connectivity in patients with FD compared to HC, which validates FD as a disorder of gut-brain interaction.

Altered connectivity of the ventrolateral prefrontal cortex – a region implicated in reward valuation and pain modulation – with other emotional-arousal, salience, executive, and central autonomic network regions was found to be a unique brain feature in FD. Moreover, assessment of the global organization of brain connectivity networks through application of graph theoretical analysis pointed toward an overall altered network topology between FD and HC. This was further substantiated by a near-perfect classification of patients and controls based on this topological analysis. These findings corroborate the results from multiple studies that reported on functional brain alterations in FD (reviewed in[33-36]), supporting the concept that the pathogenesis of this disorder likely involves a combination of central and peripheral impairments. However, this study is the first to integrate brain connectivity measurements with microbial metabolite profiles – particularly the tryptophan metabolite IAA – in a translational hypothesis-driven fashion. Indeed, the graph measures partial least squares regression model explained a substantial portion of the variation in urinary IAA levels. Of note, brain connectivity was not linked to propionate or kynurenine concentrations, indicating a specific effect for IAA. Although causality cannot be inferred from this cross-sectional study, statistical mediation analysis suggested that elevated IAA might be driven by the observed brain connectivity changes in FD. In addition, this translates the preclinical findings by Wei *et al*. of increased IAA levels in various mouse models of psychological stress[16], to a human context of a disorder where psychological stress is thought to play an important role.

Some limitations inherent to the design of the study should be acknowledged. This study applied targeted metabolomics, measuring a limited number of AAA and their metabolites, leaving other potentially relevant metabolites unexplored. However, the targeted metabolomics approach ensured an optimized and validated analysis of several key tryptophan metabolites implicated in gut-brain communication, as well as the major SCFA, in multiple human samples. Our microbial analysis was conducted by 16S rRNA gene sequencing. Future studies using higher resolution metagenomic sequencing should focus on identifying the pathways underlying these observed metabolomic alterations. In the current study, fMRI was restricted to resting state measurements, whereas task-based imaging could identify alterations in connectivity and activity in specific disorder-related contexts including stress, anxiety or pain. Lastly, findings from this relatively small single-center study should be confirmed in larger and diverse populations, controlling for the effects of geography and diet. Nevertheless, current metabolite analyses were adjusted for major dietary confounders including protein and fiber intake, as assessed by validated food frequency questionnaires, as well as PPI intake – a prevalent and important confounder.

Taken together, our study is the first to integrate peripheral microbiota-related alterations with central functionality in FD, adding to the growing body of evidence for a disturbed microbiota-gut-brain axis in FD. The first human data on alterations in tryptophan and short-chain fatty metabolism in FD – linked to its typical symptomatology – suggest they can be actionable targets in this difficult-to-treat disorder to restore microbiota-gut-brain homeostasis by dietary, probiotic or prebiotic intervention, which deserves continued investigation.

Figure legends

Figure 1: High comorbid psychological symptom burden in FD. Between-group differences in gastrointestinal (LPDS, PAGI-SYM) and psychological (GAD7, VSI, PSQ9, PHQ12, PSS, PTSD, PANAS+, PANAS-) symptoms. Linear regression models with 'PPI intake' nested in the grouping variable. *P* values represent main group effects.

Figure 2: Patients with FD exhibit a distinct amino acid metabolite profile. (**A**) Aromatic amino acids (AAA) and AAA metabolites included in the targeted metabolomics approach. Tryptophan and its metabolites are underlined. Principal component analysis of (**B**) serum AAA and AAA metabolites, and (**C**) urinary microbial AAA metabolites. Permutational analysis of variance (PERMANOVA, 10,000 permutations) quantified explained proportion of variance (R^2) by 'Group'. Between-group differences in standardized concentrations of AAA and AAA metabolites aggregated per origin, measured in (**D**) serum and (**E**) urine, (**F**) and levels of selected individual AAA metabolites. Linear regression with main 'Group' effect and 'PPI intake' nested in the grouping variable, adjusted for protein intake. *P* values represent main 'Group' effects (**D**-**F**).

Figure 3: Reduced plasma propionate levels in patients with FD. Between-group differences in concentrations of individual and total short-chain fatty acids (SCFA) measured in (**A**) feces and (**B**) plasma. Linear regression with main 'Group' effect and 'PPI intake' nested in the grouping variable, adjusted for fiber intake. *P* values represent main 'Group' effects.

Figure 4: IAA, propionate and Kyn are associated with gastrointestinal and comorbid psychological symptoms in FD. (**A**) Heatmap of associations between symptom scores and metabolites. Color scale depicts Spearman correlation coefficients. Benjamini-Hochberg adjusted significance depicted as open ($q_{FDR} < 0.1$) or filled circles ($q_{FDR} < 0.05$). Linear relationships between psychological (GAD7, PSQ9, PHQ12) and gastrointestinal (LPDS) symptom scores with (**B**) urinary indole-3-acetate (IAA), (**C**) plasma propionate, and (**D**) serum kynurenine (Kyn). (**E**) Heatmap of pairwise correlations between significantly altered metabolites of interest in FD. Color scale and values depict Spearman correlation coefficients. (**F**) Multiple linear regression analysis between significantly altered metabolites of interest in FD and symptom scores with correction for fiber and protein intake. Circle sizes correspond to Benjamini-Hochberg adjusted *P* values (q_{FDR}). Color scale depicts effect sizes (η_p^2).

Figure 5: The fecal microbiota in FD is similar compared to HC and shaped by intestinal transit time. (**A**) Distribution of stool sample consistency types between FD and

HC (Bristol Stool Scale, BSS). (**B**) Fecal microbial load (flow cytometric microbial cell counts) comparison between groups (left) or BSS category (right). (**C**) Differences in fecal microbial alpha diversity indices (genus-level) between groups. (**D**) Principal coordinate analysis (PCoA, Bray-Curtis) of fecal microbiota in FD and HC. Permutational analysis of variance (PERMANOVA, 10,000 permutations) quantified explained proportion of variance (R^2) by 'Group'. (**E**) Absolute abundance of ten most abundant fecal bacterial genera. (**F**) Univariable (between-group differences) and multivariable (between-group differences controlled for proton pump inhibitor (PPI) intake and intestinal transit time (BSS)) fecal microbial genera abundance analysis. Circle sizes correspond to Benjamini-Hochberg adjusted *P* values (q_{FDR}). Color scale depicts individual effect sizes.

Figure 6: Resting-state functional brain connectivity is altered in FD and mediates elevated urinary IAA levels. (**A**) Between-group difference in region-of-interest (ROI)-to-ROI-based connectivity for the right inferior frontal gyrus (IFG) – pars triangularis (ventrolateral prefrontal cortex, vlPFC). (**B**) Between-group difference in whole-brain voxel-based connectivity for the left vlPFC (arrow). (**C**) Difference in connectivity pattern of the left vlPFC cluster with other brain regions between FD (red) and HC (blue). (**D**) Receiver operating characteristic (ROC) curve and area under the curve (AUC) depicting the performance of brain connectivity network partial least squares discriminant analysis (PLS-DA) classification between patients with FD and HC. (**E**) Mediation of between-group differences on urinary indole-3-acetate (IAA) levels. Significant between-group effect on brain connectivity ("Path A") and significant association of brain connectivity with urinary IAA ("Path B"). Introducing brain connectivity (resting-state functional magnetic resonance imaging (fMRI)-based graph measures factor 1) as mediator of the between-group effect on urinary IAA reduced the significance of the direct between-group effect on urinary IAA ("Path C"), while the indirect through the mediator ("Path A*B") remained significant. Model outcomes of the individual mediation paths are summarized as estimate (β) ± standard error (SE) with corresponding bootstrapped 95% confidence intervals (CI).

Acknowledgements

The authors thank all the patients and volunteers for their participation in this study. We thank the personnel of the Endoscopy and Motility unit at the University Hospitals Leuven campus Gasthuisberg for their assistance with clinical study visits, in particular Karlien Geboers and Lieselot Holvoet. The authors thank Leen Rymenans, Chloë Verspecht and Thi Thuy Duyen Nguyen for their contribution to sample analysis. Icons in Figure 2B-C and Supplementary Figure 1A-B were exported with license to publish from BioRender.com.

Funding

M.C. was supported by a postdoctoral fellowship of the Belgian American Educational Foundation (BAEF). L.W. was supported by Flanders Research Foundation (FWO Vlaanderen) through a doctoral fellowship (1190619N). N.W. is a postdoctoral fellow supported by a KU Leuven C2 grant (C2M/25/041). R.Y.T. and B.D are funded by a postdoctoral fellowship from the Research Fund–Flanders. A.V.V. is a postdoctoral researcher supported by a Marie-Curie grant (HORIZON-MSCA-2023). J.T. is supported by a KU Leuven Methusalem grant (EZX-C9725-METH/14/05). L.V.O. is a research professor of the KU Leuven Special Research Fund. T.V. is a senior clinical researcher supported by the Research Fund-Flanders (FWO, 1830517N), an FWO research grant (G059822N) and a grant from the Clinical Research Fund UZ Leuven (KOOR project financiering). The Raes lab is supported by KU Leuven, VIB and the Rega Institute. This study was supported by a grant of the Biocodex Microbiota Foundation (BMF Belux 2018) and a grant of the clinical research fund (KOOR) of the University Hospitals Leuven. The funder did not influence the results/outcomes of the study despite author affiliations with the funder.

Ethical approval statement

The study was approved by the University Hospitals / KU Leuven Ethics Committee for Research (S60953, S60984) and registered at ClinicalTrials.gov (NCT03545243). All participants provided written informed consent before the start of the study. The study was conducted in accordance with the Declaration of Helsinki and the Guidelines for Good Clinical Practice. All co-authors had access to the study data and have reviewed and approved the final manuscript.

References

1. Stanghellini V, Chan FK, Hasler WL, et al. Gastroduodenal Disorders. Gastroenterology 2016;150:1380-92.
2. Sperber AD, Bangdiwala SI, Drossman DA, et al. Worldwide Prevalence and Burden of Functional Gastrointestinal Disorders, Results of Rome Foundation Global Study. Gastroenterology 2021;160:99-114.
3. Drossman DA, Hasler WL. Rome IV-functional GI disorders: disorders of gut-brain interaction. Gastroenterology 2016;150:1257-61.
4. Aro P, Talley NJ, Agréus L, et al. Functional dyspepsia impairs quality of life in the adult population. Aliment Pharmacol Ther 2011;33:1215-24.
5. Trindade IA, Hreinsson JP, Melchior C, et al. Global Prevalence of Psychological Distress and Comorbidity With Disorders of Gut-Brain Interactions. Am J Gastroenterol 2024;119:165-175.
6. Lacy BE, Weiser KT, Kennedy AT, et al. Functional dyspepsia: the economic impact to patients. Aliment Pharmacol Ther 2013;38:170-7.
7. Shah A, Fairlie T, Brown G, et al. Duodenal Eosinophils and Mast Cells in Functional Dyspepsia: A Systematic Review and Meta-Analysis of Case-Control Studies. Clin Gastroenterol Hepatol 2022;20:2229-2242.e29.
8. Vanheel H, Vicario M, Vanuytsel T, et al. Impaired duodenal mucosal integrity and low-grade inflammation in functional dyspepsia. Gut 2014;63:262-71.
9. Zhong L, Shanahan ER, Raj A, et al. Dyspepsia and the microbiome: time to focus on the small intestine. Gut 2017;66:1168-9.
10. Fukui A, Takagi T, Naito Y, et al. Higher levels of Streptococcus in upper gastrointestinal mucosa associated with symptoms in patients with functional dyspepsia. Digestion 2020;101:38-45.
11. Shanahan ER, Kang S, Staudacher H, et al. Alterations to the duodenal microbiota are linked to gastric emptying and symptoms in functional dyspepsia. Gut 2023;72:929-938.
12. Wauters L, Tito RY, Ceulemans M, et al. Duodenal Dysbiosis and Relation to the Efficacy of Proton Pump Inhibitors in Functional Dyspepsia. Int J Mol Sci 2021;22.
13. Jones MP, Tack J, Van Oudenhove L, et al. Mood and Anxiety Disorders Precede Development of Functional Gastrointestinal Disorders in Patients but Not in the Population. Clin Gastroenterol Hepatol 2017;15:1014-1020.e4.
14. Dalile B, Van Oudenhove L, Vervliet B, et al. The role of short-chain fatty acids in microbiota-gut-brain communication. Nat Rev Gastroenterol Hepatol 2019;16:461-478.

15. Gheorghe CE, Martin JA, Manriquez FV, et al. Focus on the essentials: tryptophan metabolism and the microbiome-gut-brain axis. Curr Opin Pharmacol 2019;48:137-145.
16. Wei W, Liu Y, Hou Y, et al. Psychological stress-induced microbial metabolite indole-3-acetate disrupts intestinal cell lineage commitment. Cell Metab 2024;36:466-483.e7.
17. Lewis SJ, Heaton KW. Stool form scale as a useful guide to intestinal transit time. Scand J Gastroenterol 1997;32:920-4.
18. de Loor H, Poesen R, De Leger W, et al. A liquid chromatography - tandem mass spectrometry method to measure a selected panel of uremic retention solutes derived from endogenous and colonic microbial metabolism. Anal Chim Acta 2016;936:149-56.
19. Dalile B, Vervliet B, Bergonzelli G, et al. Colon-delivered short-chain fatty acids attenuate the cortisol response to psychosocial stress in healthy men: a randomized, placebo-controlled trial. Neuropsychopharmacology 2020;45:2257-2266.
20. Powers L, Osborn MK, Yang D, et al. Assay of the concentration and stable isotope enrichment of short-chain fatty acids by gas chromatography/mass spectrometry. Journal of Mass Spectrometry 1995;30:747-754.
21. Wauters L, Ceulemans M, Frings D, et al. Proton pump inhibitors reduce duodenal eosinophilia, mast cells and permeability in patients with functional dyspepsia. Gastroenterology 2021;160:1521-31.
22. Vandeputte D, Kathagen G, D'Hoe K, et al. Quantitative microbiome profiling links gut community variation to microbial load. Nature 2017;551:507-511.
23. Oishi K, Faria A, Jiang H, et al. Atlas-based whole brain white matter analysis using large deformation diffeomorphic metric mapping: application to normal elderly and Alzheimer's disease participants. Neuroimage 2009;46:486-99.
24. Collins SM, Surette M, Bercik P. The interplay between the intestinal microbiota and the brain. Nat Rev Microbiol 2012;10:735-42.
25. Mayer EA, Tillisch K, Gupta A. Gut/brain axis and the microbiota. J Clin Invest 2015;125:926-38.
26. Cryan JF, Dinan TG. Mind-altering microorganisms: the impact of the gut microbiota on brain and behaviour. Nat Rev Neurosci 2012;13:701-12.
27. Li M, Ding Y, Wei J, et al. Gut microbiota metabolite indole-3-acetic acid maintains intestinal epithelial homeostasis through mucin sulfation. Gut Microbes 2024;16:2377576.

28. Schiweck C, Dalile B, Balliet A, et al. Circulating short chain fatty acids are associated with depression severity and predict remission from major depressive disorder. Brain Behav Immun Health 2025;48:101070.
29. Kim SH, Choi Y, Oh J, et al. Associations among the Duodenal Ecosystem, Gut Microbiota, and Nutrient Intake in Functional Dyspepsia. Gut Liver 2024;18:621-631.
30. Malan-Müller S, Valles-Colomer M, Palomo T, et al. The gut-microbiota-brain axis in a Spanish population in the aftermath of the COVID-19 pandemic: microbiota composition linked to anxiety, trauma, and depression profiles. Gut Microbes 2023;15:2162306.
31. Wauters L, Slaets H, De Paepe K, et al. Efficacy and safety of spore-forming probiotics in the treatment of functional dyspepsia: a pilot randomised, double-blind, placebo-controlled trial. Lancet Gastroenterol Hepatol 2021;6:784-792.
32. Zhang Q, Li G, Zhao W, et al. Efficacy of Bifidobacterium animalis subsp. lactis BL-99 in the treatment of functional dyspepsia: a randomized placebo-controlled clinical trial. Nat Commun 2024;15:227.
33. Kano M, Dupont P, Aziz Q, et al. Understanding Neurogastroenterology From Neuroimaging Perspective: A Comprehensive Review of Functional and Structural Brain Imaging in Functional Gastrointestinal Disorders. J Neurogastroenterol Motil 2018;24:512-527.
34. Lee IS, Wang H, Chae Y, et al. Functional neuroimaging studies in functional dyspepsia patients: a systematic review. Neurogastroenterol Motil 2016;28:793-805.
35. Mao Y, Zhang P, Sun R, et al. Altered resting-state brain activity in functional dyspepsia patients: a coordinate-based meta-analysis. Front Neurosci 2023;17:1174287.
36. Sun R, Zhou J, Qu Y, et al. Resting-state functional brain alterations in functional dyspepsia: Protocol for a systematic review and voxel-based meta-analysis. Medicine (Baltimore) 2020;99:e23292.

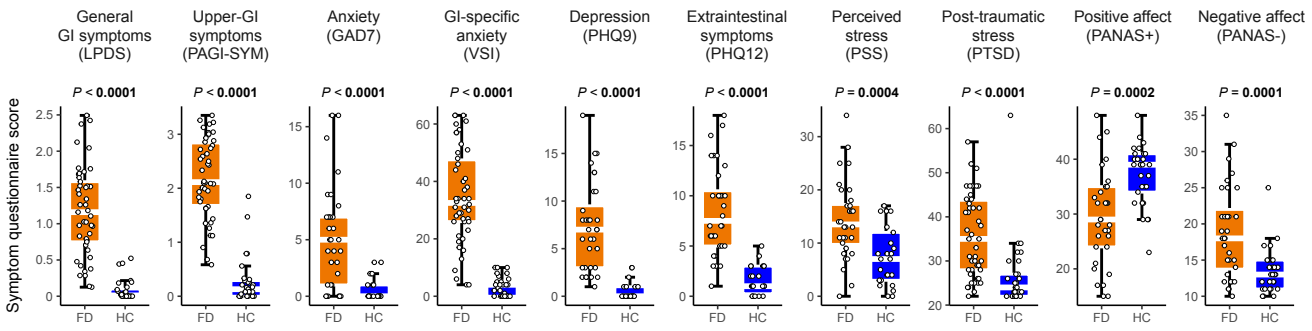
General GI symptoms (LPDS)
Upper-GI symptoms (PAGI-SYM)
Anxiety (GAD7)
GI-specific anxiety (VSI)
Depression (PHQ9)
Extraintestinal symptoms (PHQ12)
Perceived stress (PSS)
Post-traumatic stress (PTSD)
Positive affect (PANAS+)
Negative affect (PANAS-)
Symptom questionnaire score
P < 0.0001
P < 0.0001
P < 0.0001
P < 0.0001
P < 0.0001
P < 0.0001
P = 0.0004
P < 0.0001
P = 0.0002
P = 0.0001
FD
HC

Figure 1

A

Molecule	Type
Phenylalanine (Phe)	Aromatic amino acids (AAA)
Tyrosine (Tyr)	
Tryptophan (Trp)	
p-Cresyl glucuronide (pCG)	Microbial AAA metabolites
p-Cresyl sulfate (pCS)	
Phenyl glucuronide (PhG)	
Phenyl sulfate (PhS)	
Phenylacetylglutamine (PAGln)	
Indole-3-acetate (IAA)	
Indoxyl sulfate (IxS)	
Hippuric acid (HA)	
Kynurenine (Kyn)	Host AAA metabolites
Kynurenic acid (KA)	
Trimethylamine N-oxide (TMAO)	Miscellaneous metabolites
3-carboxy-4-methyl-5-propyl-2-furanpropanoic acid (CMPF)	

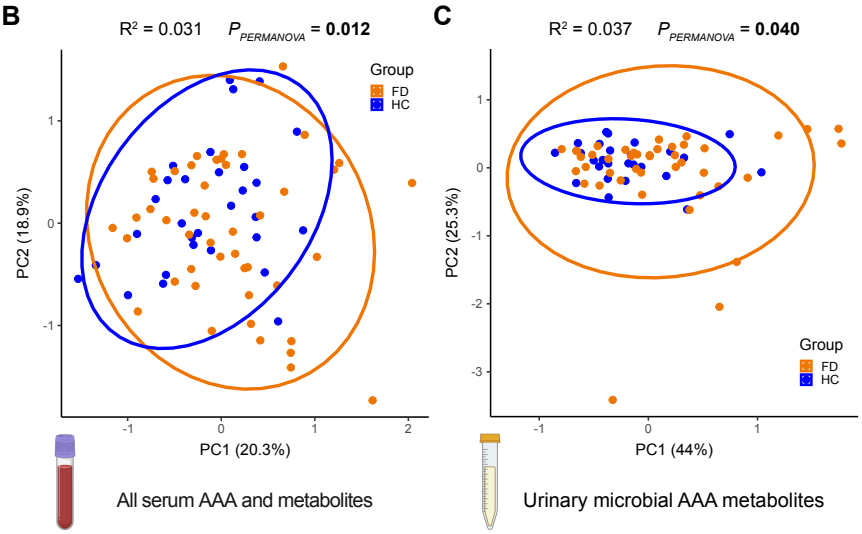

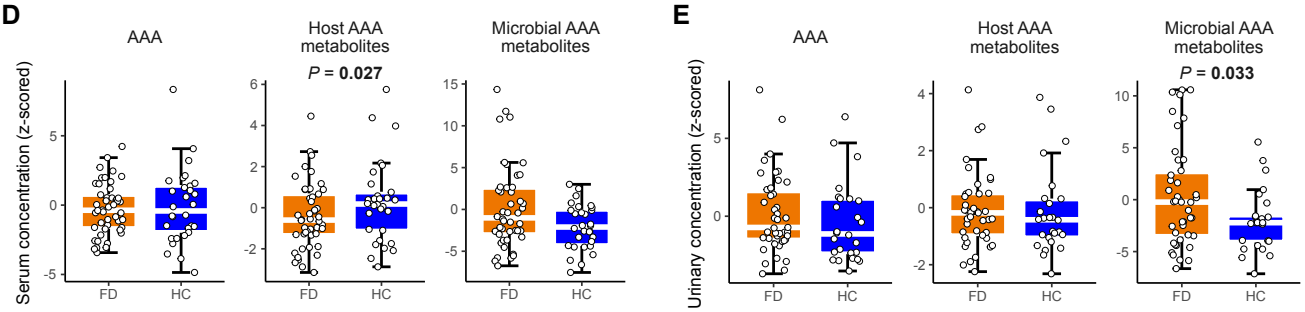

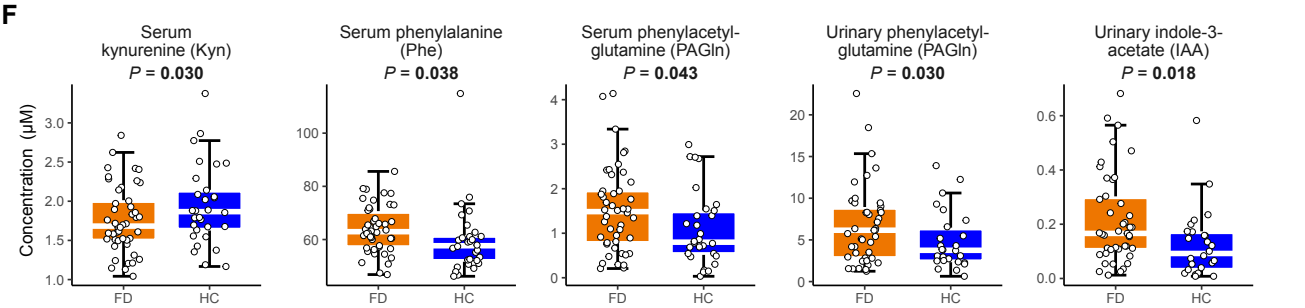

Figure 2

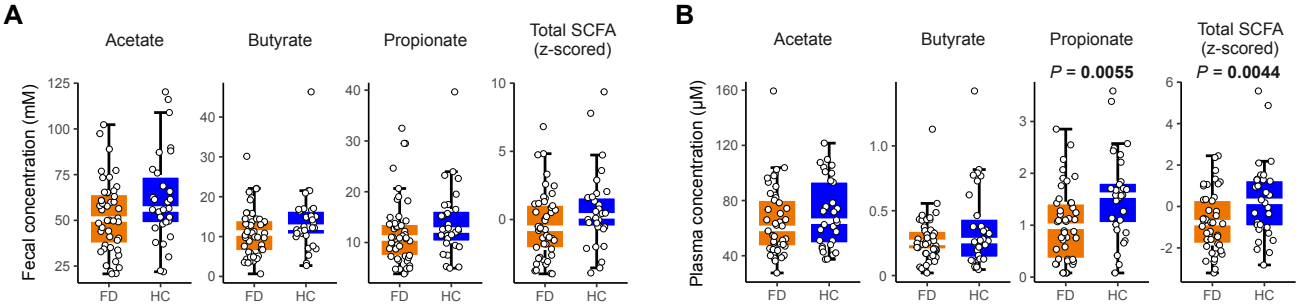
A
Acetate
Butyrate
Propionate
Total SCFA
(z-scored)
Fecal concentration (mM)
FD
HC
B
Plasma concentration (μM)
P = 0.0055
P = 0.0044

Figure 3

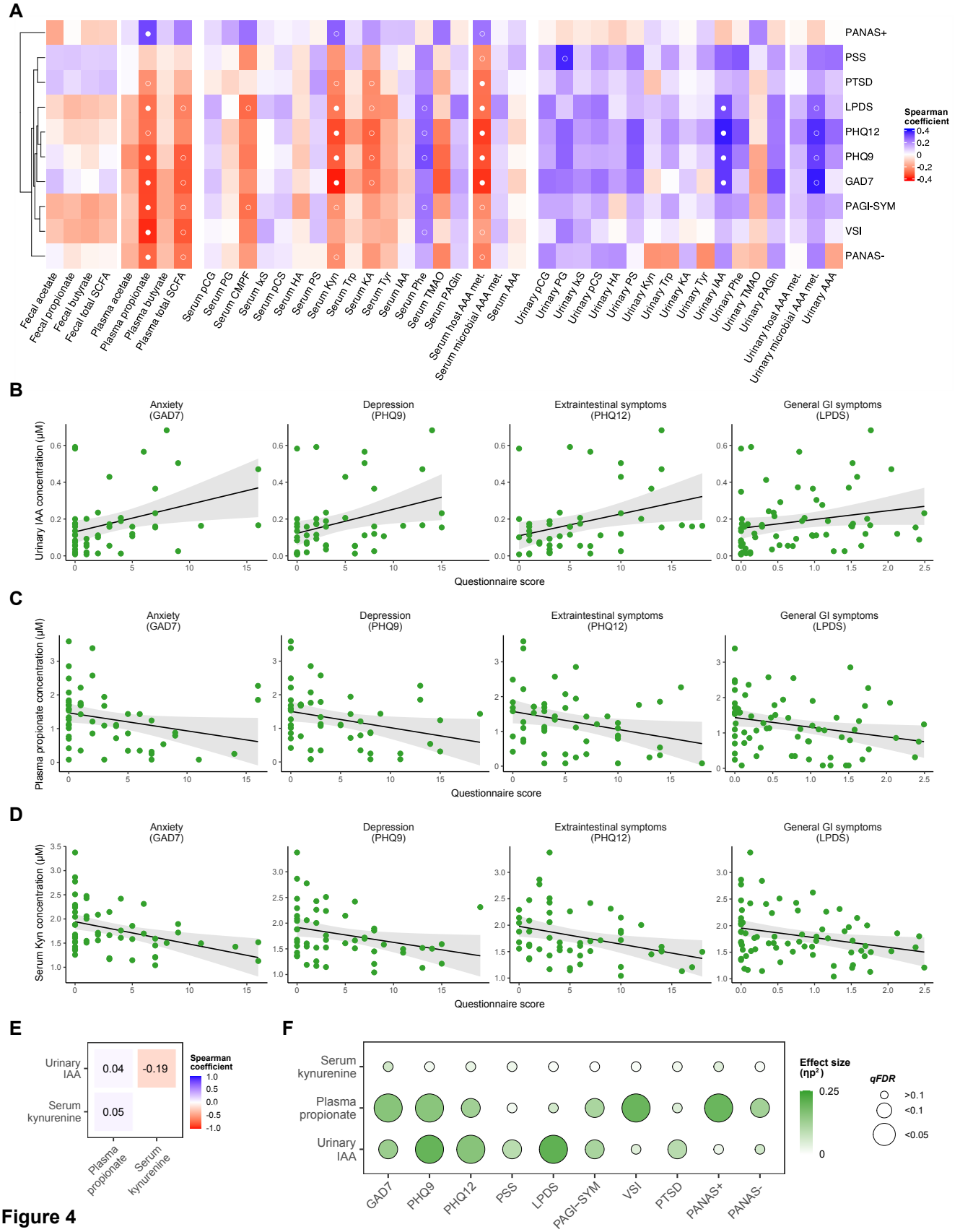
A
PANAS+
PSS
PTSD
LPDS
PHQ12
PHQ9
GAD7
PAGI-SYM
VSI
PANAS-
Spearman coefficient
0.4
0.2
0
-0.2
-0.4
Fecal acetate
Fecal propionate
Fecal butyrate
Fecal total SCFA
Plasma acetate
Plasma propionate
Plasma butyrate
Plasma total SCFA
Serum pCG
Serum PG
Serum CMPF
Serum kS
Serum pCS
Serum HA
Serum PS
Serum Kyn
Serum Trp
Serum KA
Serum Tyr
Serum IAA
Serum Phe
Serum TMAO
Serum PAGln
Serum host AAA met.
Serum microbial AAA met.
Serum AAA
Urinary pCG
Urinary PG
Urinary kS
Urinary pCS
Urinary HA
Urinary PS
Urinary Kyn
Urinary Trp
Urinary KA
Urinary Tyr
Urinary IAA
Urinary Phe
Urinary TMAO
Urinary PAGln
Urinary host AAA met.
Urinary microbial AAA met.
Urinary AAA
B
Anxiety (GAD7)
Depression (PHQ9)
Extraintestinal symptoms (PHQ12)
General GI symptoms (LPDS)
Urinary IAA concentration (µM)
Questionnaire score
C
Anxiety (GAD7)
Depression (PHQ9)
Extraintestinal symptoms (PHQ12)
General GI symptoms (LPDS)
Plasma propionate concentration (µM)
Questionnaire score
D
Anxiety (GAD7)
Depression (PHQ9)
Extraintestinal symptoms (PHQ12)
General GI symptoms (LPDS)
Serum Kyn concentration (µM)
Questionnaire score
E
Urinary IAA
Serum kynurenine
0.04
-0.19
0.05
Plasma propionate
Serum kynurenine
Spearman coefficient
1.0
0.5
0.0
-0.5
-1.0
F
Serum kynurenine
Plasma propionate
Urinary IAA
GAD7
PHQ9
PHQ12
PSS
LPDS
PAGI-SYM
VSI
PTSD
PANAS+
PANAS-
Effect size (ηp²)
0.25
0
qFDR
>0.1
<0.1
<0.05

Figure 4

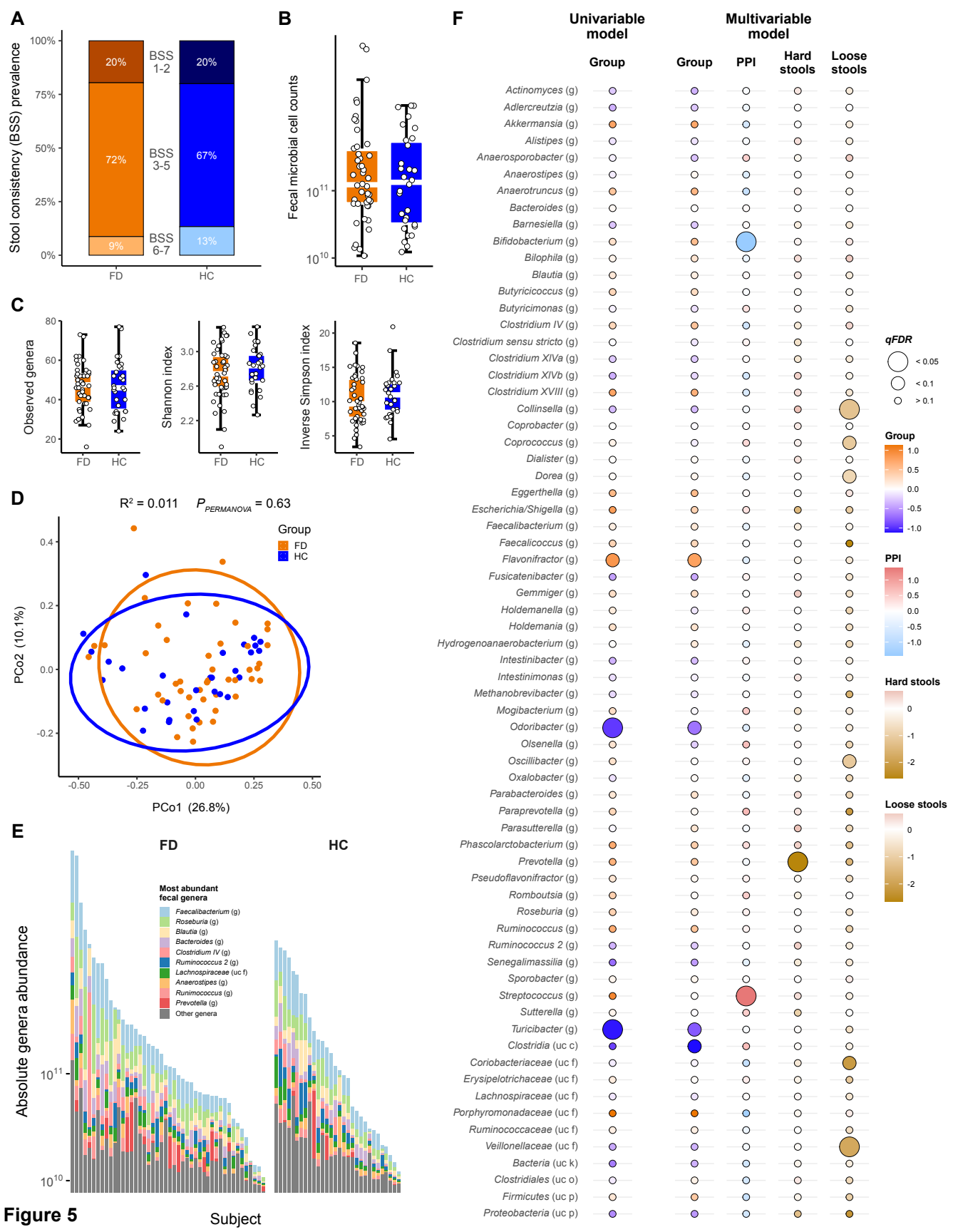
A
Stool consistency (BSS) prevalence
100%
75%
50%
25%
0%
20%
72%
9%
20%
67%
13%
BSS 1-2
BSS 3-5
BSS 6-7
FD
HC
B
Fecal microbial cell counts
10^{11}
10^{10}
FD
HC
C
Observed genera
Shannon index
Inverse Simpson index
FD
HC
D
$R^2 = 0.011$ $P_{PERMANOVA} = 0.63$
Group
FD
HC
PCo2 (10.1%)
PCo1 (26.8%)
E
FD
HC
Most abundant fecal genera
Faecalibacterium (g)
Roseburia (g)
Blautia (g)
Bacteroides (g)
Clostridium IV (g)
Ruminococcus 2 (g)
Lachnospiraceae (uc f)
Anaerostipes (g)
Runimococcus (g)
Prevotella (g)
Other genera
Absolute genera abundance
10^{11}
10^{10}
Subject
F
Univariable model
Multivariable model
Group
Group
PPI
Hard stools
Loose stools
Actinomyces (g)
Adlercreutzia (g)
Akkermansia (g)
Alistipes (g)
Anaerosporobacter (g)
Anaerostipes (g)
Anaerotruncus (g)
Bacteroides (g)
Barnesiella (g)
Bifidobacterium (g)
Bilophila (g)
Blautia (g)
Butyricicoccus (g)
Butyricimonas (g)
Clostridium IV (g)
Clostridium sensu stricto (g)
Clostridium XIVa (g)
Clostridium XIVb (g)
Clostridium XVIII (g)
Collinsella (g)
Coprobacter (g)
Coprococcus (g)
Dialister (g)
Dorea (g)
Eggerthella (g)
Escherichia/Shigella (g)
Faecalibacterium (g)
Faecalicoccus (g)
Flavonifractor (g)
Fusicatenibacter (g)
Gemmiger (g)
Holdemanella (g)
Holdemania (g)
Hydrogenoanaerobacterium (g)
Intestinibacter (g)
Intestinimonas (g)
Methanobrevibacter (g)
Mogibacterium (g)
Odoribacter (g)
Olsenella (g)
Oscillibacter (g)
Oxalobacter (g)
Parabacteroides (g)
Paraprevotella (g)
Parasutterella (g)
Phascolarctobacterium (g)
Prevotella (g)
Pseudoflavonifractor (g)
Romboutsia (g)
Roseburia (g)
Ruminococcus (g)
Ruminococcus 2 (g)
Senegalimassilia (g)
Sporobacter (g)
Streptococcus (g)
Sutterella (g)
Turicibacter (g)
Clostridia (uc c)
Coriobacteriaceae (uc f)
Erysipelotrichaceae (uc f)
Lachnospiraceae (uc f)
Porphyromonadaceae (uc f)
Ruminococcaceae (uc f)
Veillonellaceae (uc f)
Bacteria (uc k)
Clostridiales (uc o)
Firmicutes (uc p)
Proteobacteria (uc p)
qFDR
< 0.05
< 0.1
> 0.1
Group
1.0
0.5
0.0
-0.5
-1.0
PPI
1.0
0.5
0.0
-0.5
-1.0
Hard stools
0
-1
-2
Loose stools
0
-1
-2

Figure 5

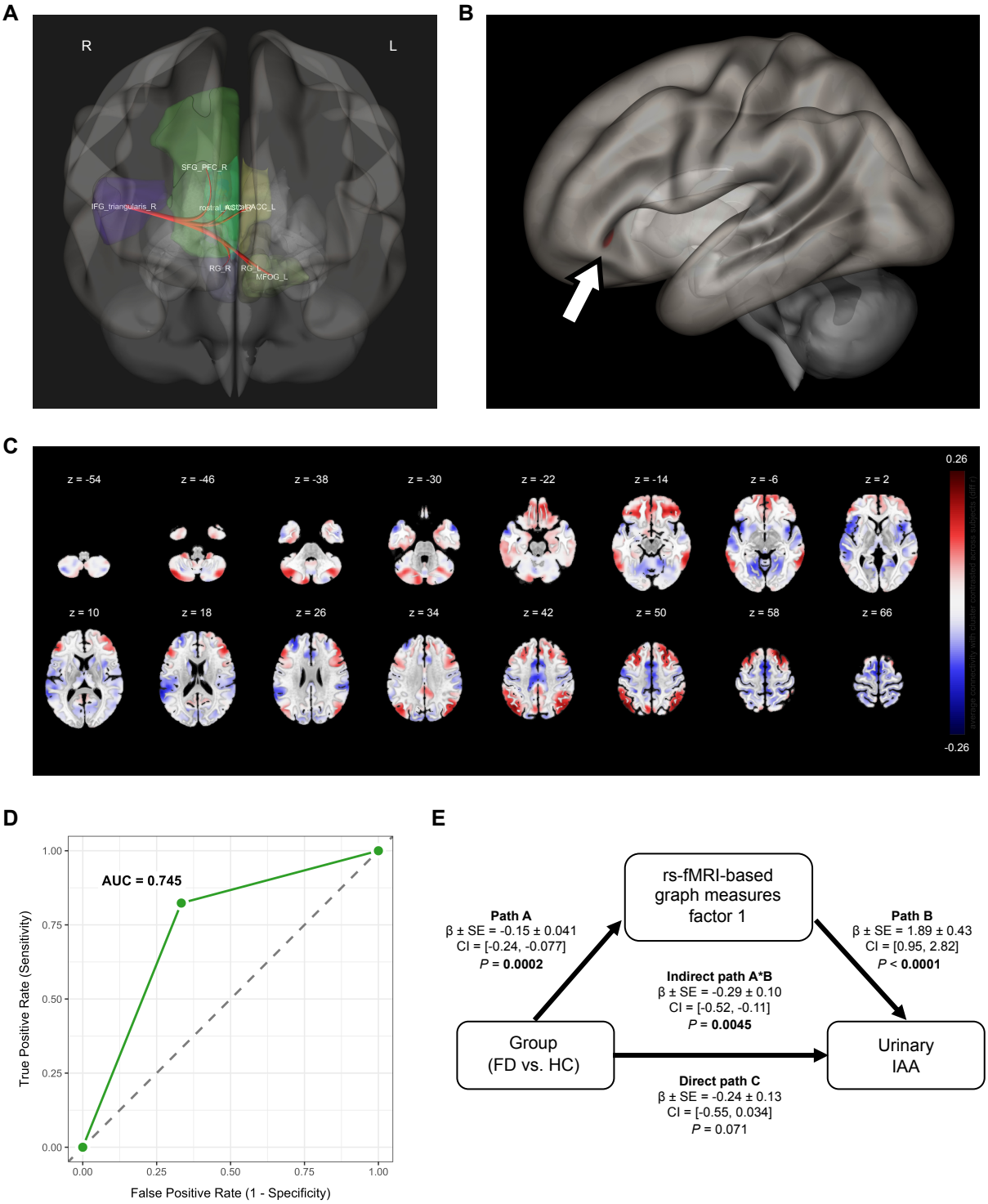
A
R
L
SFG_PFC_R
IFG_triangularis_R
rostral_ACC_R
ACC_L
RG_R
RG_L
MFOG_L
B
C
z = -54
z = -46
z = -38
z = -30
z = -22
z = -14
z = -6
z = 2
z = 10
z = 18
z = 26
z = 34
z = 42
z = 50
z = 58
z = 66
0.26
-0.26
D
AUC = 0.745
True Positive Rate (Sensitivity)
False Positive Rate (1 - Specificity)
0.00
0.25
0.50
0.75
1.00
E
rs-fMRI-based graph measures factor 1
Path A
β ± SE = -0.15 ± 0.041
CI = [-0.24, -0.077]
P = 0.0002
Path B
β ± SE = 1.89 ± 0.43
CI = [0.95, 2.82]
P < 0.0001
Indirect path A*B
β ± SE = -0.29 ± 0.10
CI = [-0.52, -0.11]
P = 0.0045
Group (FD vs. HC)
Urinary IAA
Direct path C
β ± SE = -0.24 ± 0.13
CI = [-0.55, 0.034]
P = 0.071

Figure 6